Enhancement, and Minutias Detection

Daniel Novák

11.10, 2011, Prague

Acknowledgments: Xavier Palathingal, Andrzej Drygajlo, Handbook of Fingerprint Recognition

laboratory Gerstner

Outline

- Introduction
- Segmentation
- Estimation of Local Orientation
- Estimation of Local Ridge Frequency
- Enhancement
- Minuitiae detection

laboratory Gerstner

Fingerprint

- Interleaved ridges and valleys
- Ridge width: 100 μm-300 μm
- Ridge-valley cycle: 500 μm

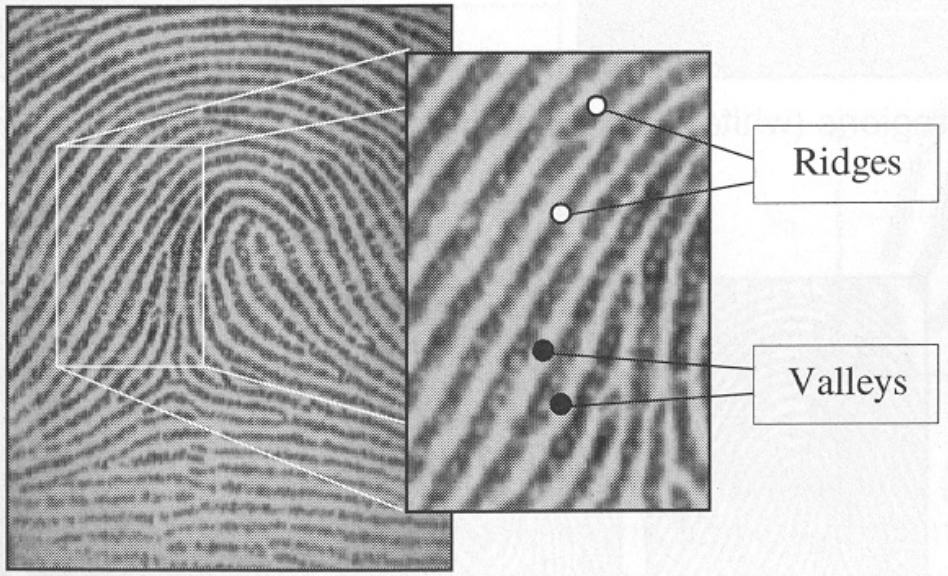

Figure 3.1. Ridges and valleys on a fingerprint image.

A Global Look

Singularities: In the global level the fingerprint pattern shows some distinct shapes

- Loop ( )
- Delta (Λ)
- Whorl (O)…Two facing loop

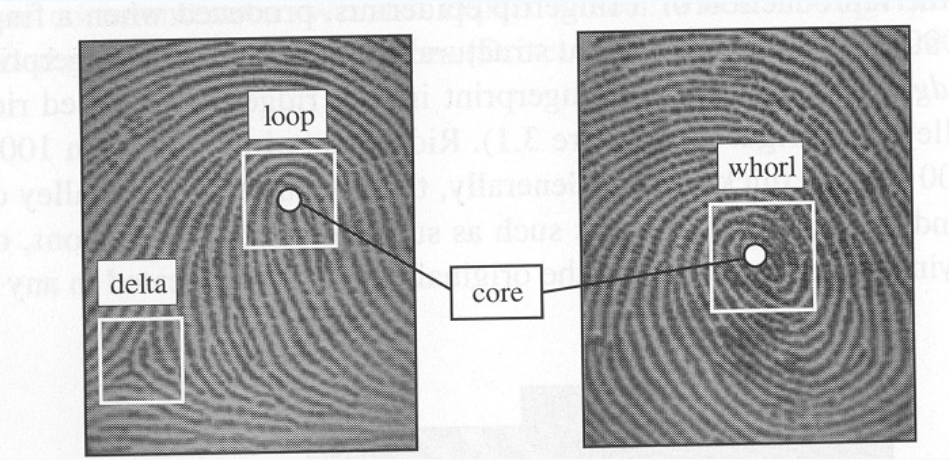

Core:

- A reference point for the alignment.
- The northmost loop type singularity.
- According to Henry(1900), it is the northmost point of the innermost ridgeline.
- Not all fingerprints have a core (Arch type fingerprints)

A Global Look

Singular regions are commonly used for fingerprint classification:

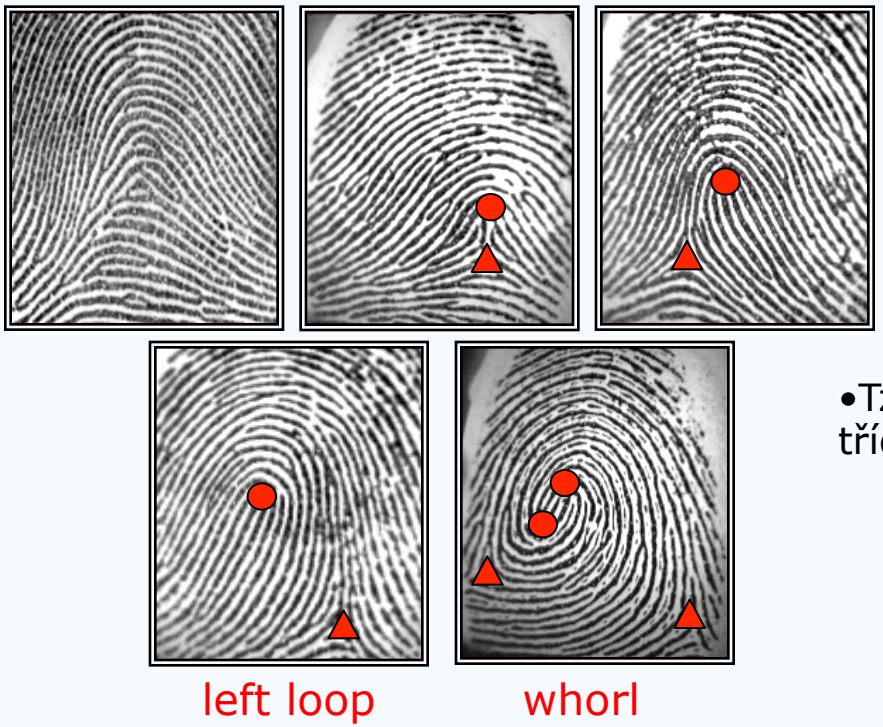

- Tzv Henryho systém, rozděluje otisky do pěti tříd
  - Závit (whorl)
  - Levá a pravá smyčka (loop)
  - Oblouk (arch)
  - Špičatý oblouk (tented arch)

Local Look

Minutia: Small details. Discontinuties in the ridges. (Sir Francis Galton)

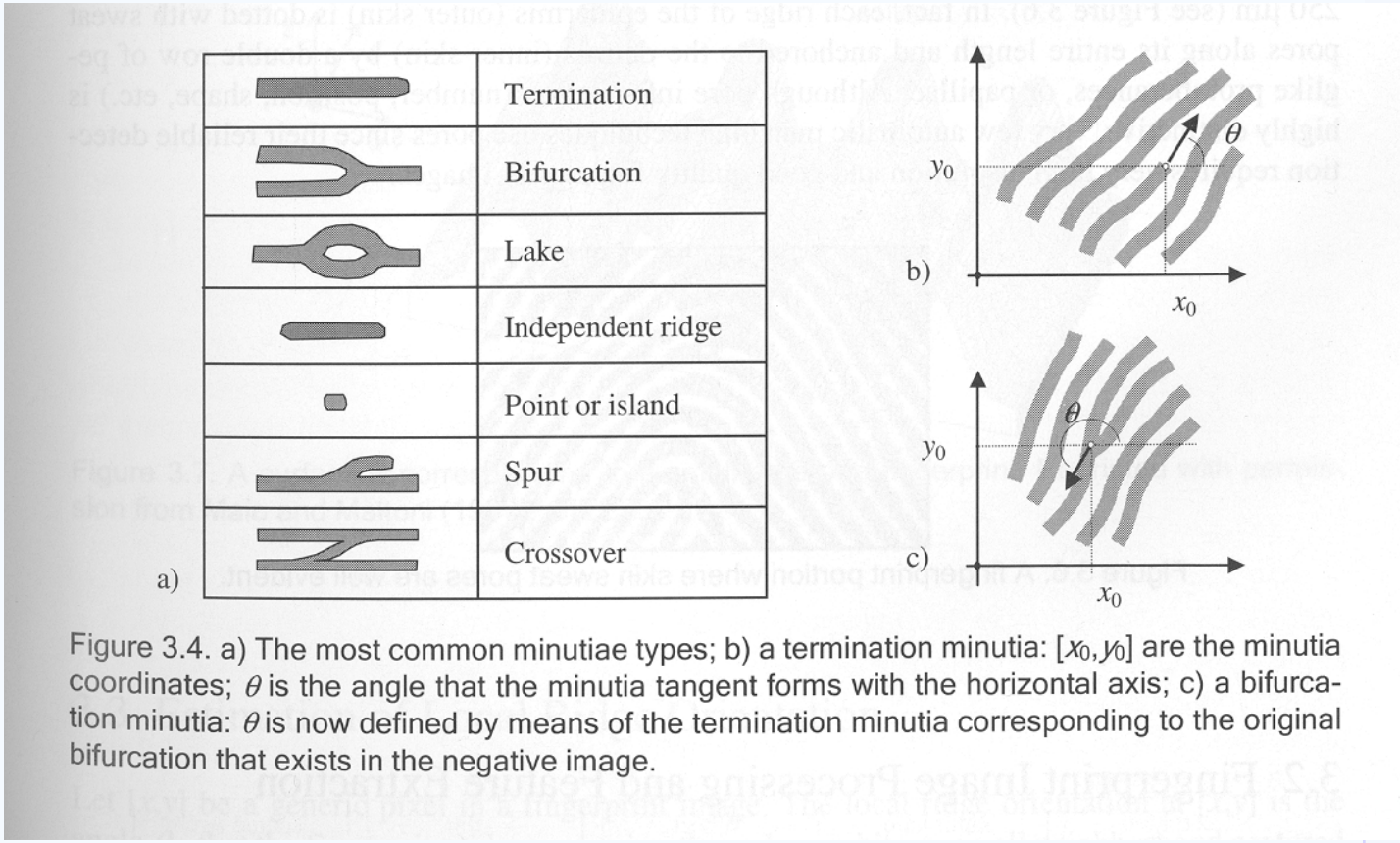

Figure 3.4. a) The most common minutiae types; b) a termination minutia: $[x_0, y_0]$ are the minutia coordinates; θ is the angle that the minutia tangent forms with the horizontal axis; c) a bifurcation minutia: θ is now defined by means of the termination minutia corresponding to the original bifurcation that exists in the negative image.

Terminologie

  - Papilarni linie
  - Vyvýšeniny (ridge)+ prohlubeniny (furrow)
- Charakteristické body
  - Kritické (singulární) body – globálně význačné body
    - Jádro
    - Delty
  - Markanty (Minutiaes) – lokálně význačné body
    - Rozvětvení (bifurcation)
    - Zakončení (ridge ending)
    - Krátké hrany (short ridge)
    - Překřížení (crossover, bridge)
    - Krátké rozvětvení (spur)
    - Očka (ridge enclosures)

laboratory Gerstner

Local Look

Ridge ending / ridge bifurcation **duality**

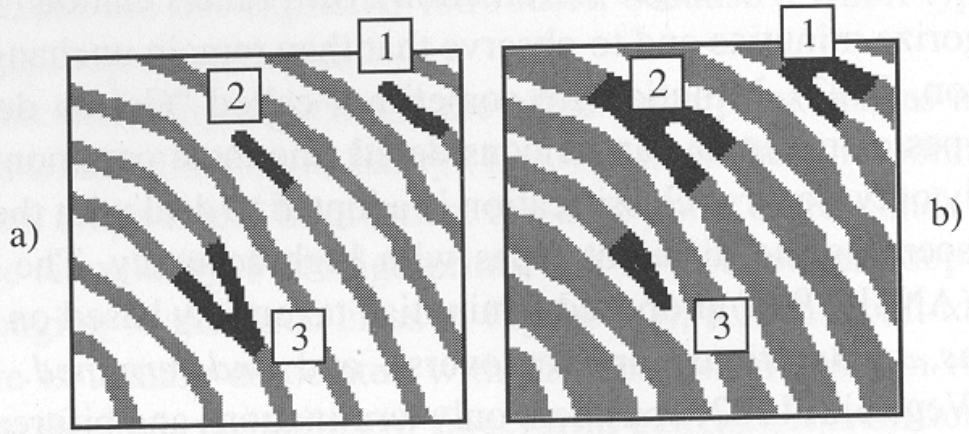

Figure 3.5. The termination/bifurcation duality on a) a binary image and b) its negative image.

Local Look

Sweat Pores

- High resolution images (1000 dpi)
- Size 60-250 μm
- Highly distinctive
- Not practical (High resolution, good quality images)

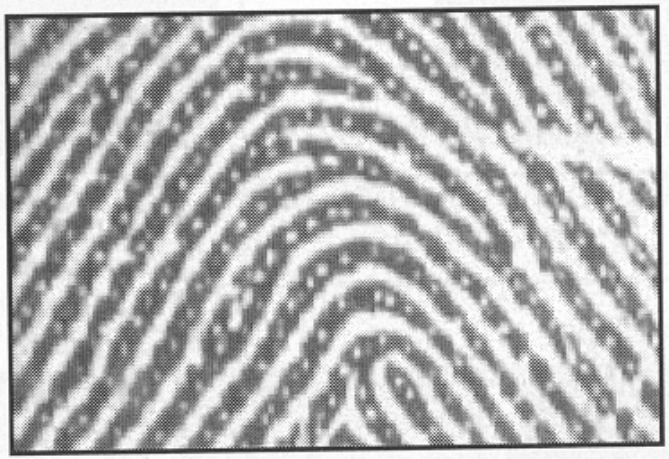

Figure 3.6. A fingerprint portion where skin sweat pores are well evident.

Segmentation

Original

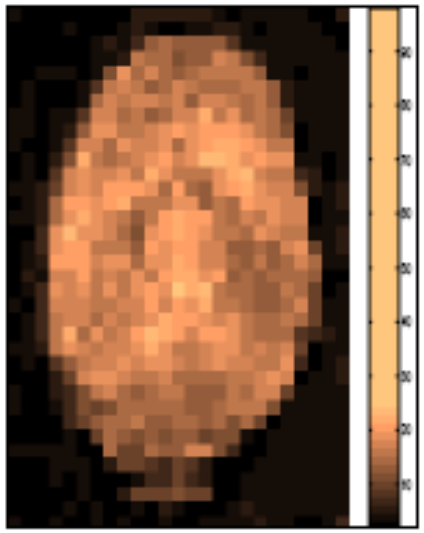

Variance image

Segmented image

Segmentation is the process of isolating foreground from background:

- Image block (16x16 pixels) decomposition
- Thresholding using variance of gradient for each block

Segmentation

- Separating FP from background
- Straited patterns: no thresholding, striped and oriented pattern & isotropic pattern without orientation
- **Segmentation Methods (16x16 block)**
  - Variance orthogonal to the ridge direction **[Ratha95]**
    - Assumption: fingerprint area will exhibit high variance, where as the background and noisy regions will exhibit low variance.
    - Variance can also be used as the quality parameter of the regions.
      - High variance (high contrast): good quality
      - Low variance (low contrast): poor quality
    - Average magnitude of gradient in blocks
      - **Fp1 = segmentimage(Fp1);**

Estimation of Local Ridge Orientation

- Average orientation around indices i,j
- Unoriented directions
- Weighted (r_{ij})
- Gradient, maximum pixel-intensity change, arctan gy/gx

$$\nabla f = \left(\frac{\partial f}{\partial x_1}, \ldots, \frac{\partial f}{\partial x_n} \right).$$

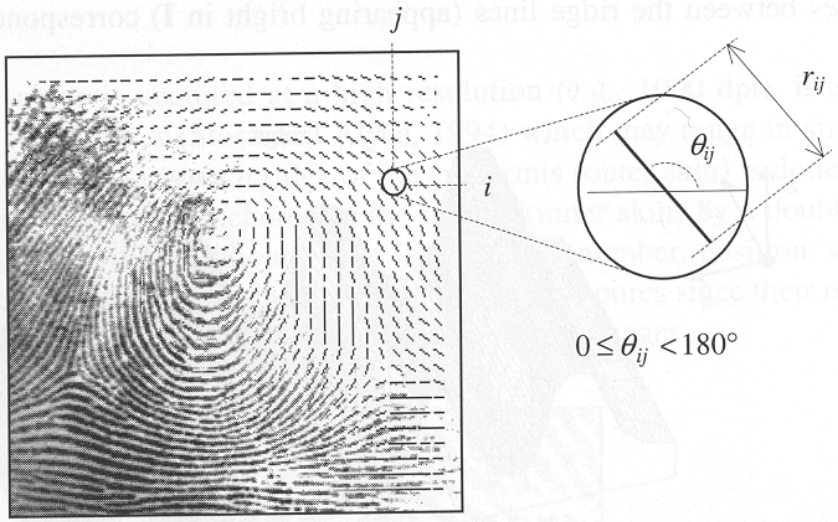

Figure 3.8. A fingerprint image faded into the corresponding orientation image computed over a square-meshed grid of size 16×16. Each element denotes the local orientation of the fingerprint ridges; the element length is proportional to its reliability.

Estimation of Local Ridge Orientation

- Simple Approach
  - Gradient with Sobel or Prewitt operators
  - Θ_{ij} is orthogonal to the direction of the gradient

$$M_x = \begin{bmatrix} -1 & 0 & 1 \\ -1 & 0 & 1 \\ -1 & 0 & 1 \end{bmatrix} \qquad M_y = \begin{bmatrix} -1 & -1 & -1 \\ 0 & 0 & 0 \\ 1 & 1 & 1 \end{bmatrix}$$

$$M_x = \begin{bmatrix} -1 & 0 & 1 \\ -2 & 0 & 2 \\ -1 & 0 & 1 \end{bmatrix} \qquad M_y = \begin{bmatrix} -1 & -2 & -1 \\ 0 & 0 & 0 \\ 1 & 2 & 1 \end{bmatrix}$$

- Drawbacks:
- Non-linear and discontinuous around 90
- A single estimate is sensitive to noise
- Circularity of angles: Averaging is not possible
- Averaging is not well defined.

laboratory Gerstner

Estimation of Local Ridge Orientation

- Averaging Gradient Estimates
  (Kass, Witkin 1987)

$$d_{ij} = [r_{ij}.cos2\theta_{ij}, r_{ij}sin2\theta_{ij}]$$

$$\overline{\mathbf{d}} = \left[\frac{1}{n^2} \sum_{i,j} r_{ij} \cdot \cos 2\theta_{ij}, \frac{1}{n^2} \sum_{i,j} r_{ij} \cdot \sin 2\theta_{ij} \right].$$

laboratory Gerstner

Estimation of Local Ridge Orientation

- Effect of averaging

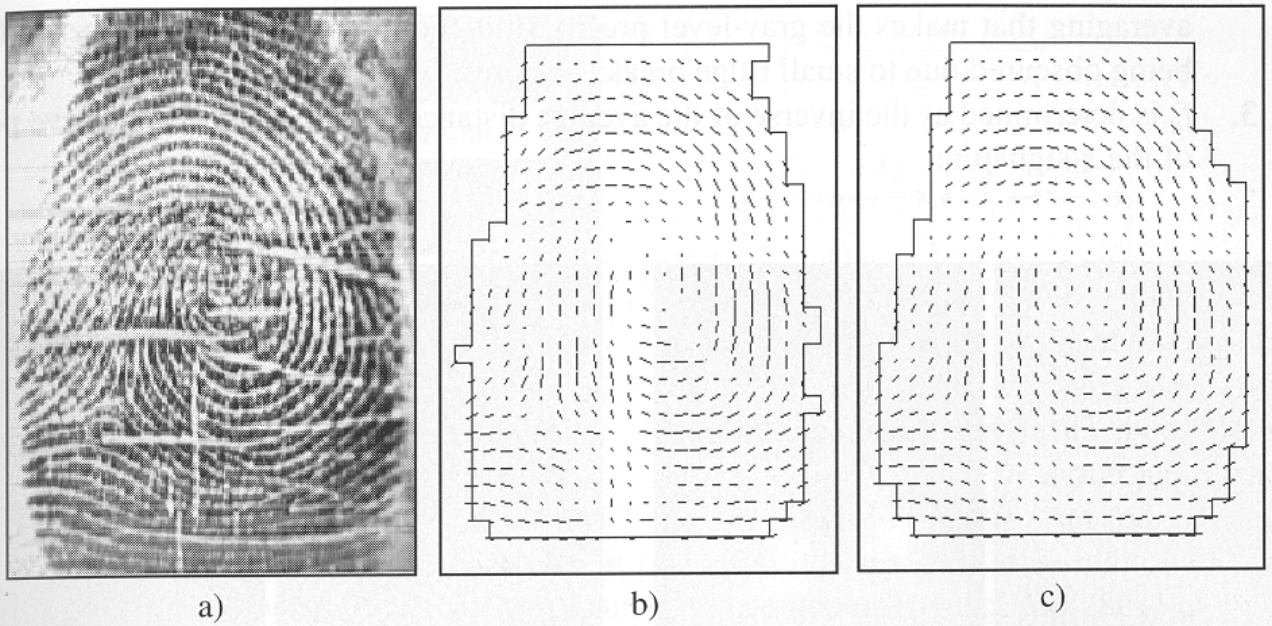

Figure 3.9. a) A poor quality fingerprint image; b) the orientation image of the fingerprint in a) is computed through the Donahue and Rokhlin (1993) method; the orientation of several elements is clearly inconsistent and a regularization step appears necessary; c) the orientation image is the result of the local averaging of each element in b) in its 3×3 window according to Equation (2).

Orientation field

An orientation is calculated for each 16x16 block

- Compute the gradient of the smoothed block. $G_x(i,j)$ and $G_y(i,j)$ using 3x3 Sobel Masks
- Obtain the dominant direction in the block using the following equation:

$$\theta_d = \frac{1}{2} tan^{-1} \left(\frac{\sum_{i=1}^{16} \sum_{j=1}^{16} 2G_x(i,j)G_y(i,j)}{\sum_{i=1}^{16} \sum_{j=1}^{16} (G_x(i,j)^2 - G_y(i,j)^2)} \right), G_x \neq 0 \text{ and } G_y \neq 0 \quad (1)$$

$$G_{xy} = \sum_{h=-8}^{8} \sum_{k=-8}^{8} \nabla_x(x_i + h, y_j + k) \cdot \nabla_y(x_i + h, y_j + k),$$

$$G_{xx} = \sum_{h=-8}^{8} \sum_{k=-8}^{8} \nabla_x(x_i + h, y_j + k)^2,$$

$$G_{yy} = \sum_{h=-8}^{8} \sum_{k=-8}^{8} \nabla_y(x_i + h, y_j + k)^2,$$

- **DEMO: Fp1 = computeorientationarray(Fp1);**
- Gradient is computed by (standard): [fx, fy] = gradient(double(im));
- Block 10x10

Example: Orientation field

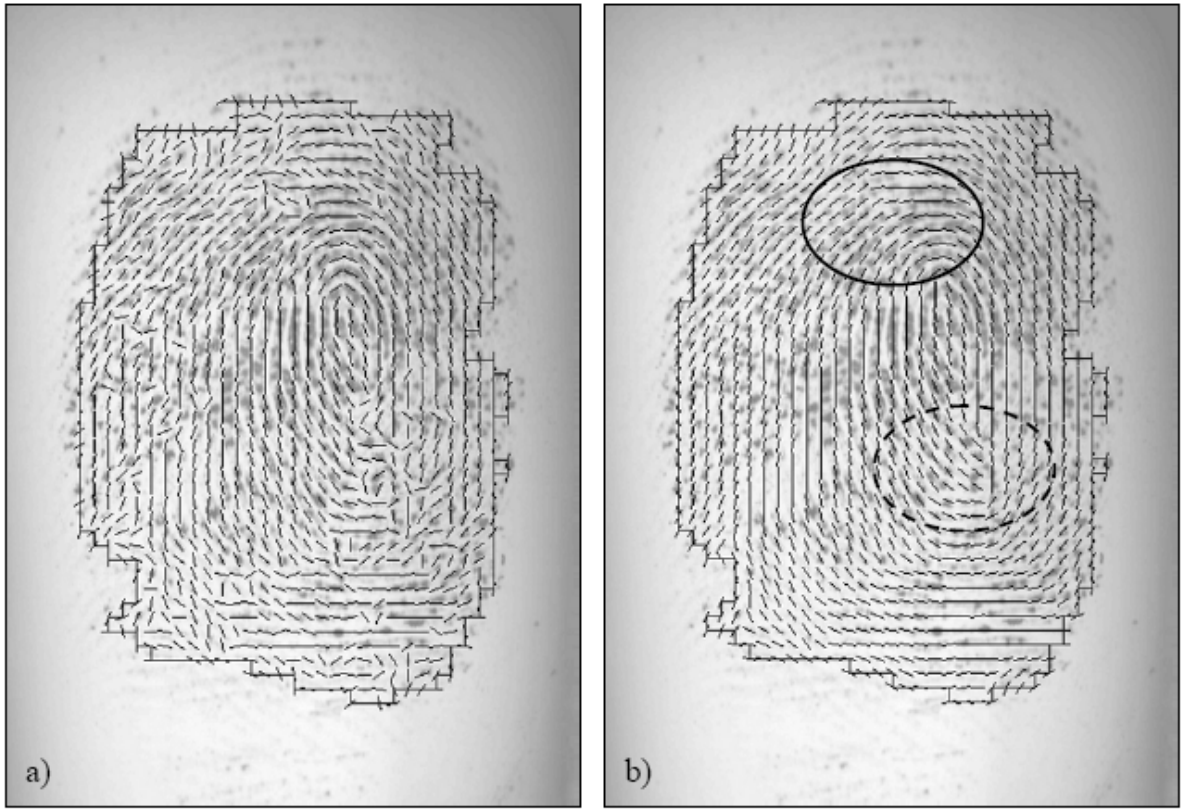

Figure 3.12. a) Estimation of local ridge orientation in a fingerprint through the gradient-based approach corresponding to Equation (3): in the noisy regions the estimation is unreliable; b) two iterations of local (3x3) smoothing are applied, resulting in a more consistent representation; it is worth noting that while the smoothing recovered the correct orientation at several places (e.g., inside the solid circle), it altered the average orientation inside the region denoted by the dashed circle where incorrect orientations were dominating the correct one.

Estimation of Local Ridge Frequency

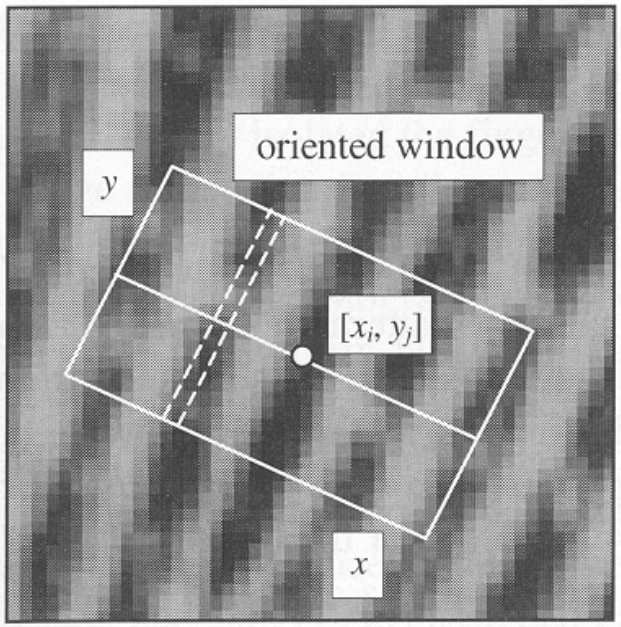

$$f_{ij} = \frac{4}{s_1 + s_2 + s_3 + s_4}$$

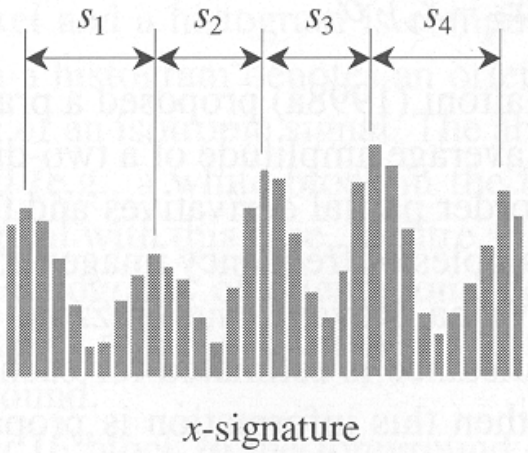

Figure 3.11. An oriented window centered at $[x_i, y_j]$; the dashed lines show the pixels whose gray-levels are accumulated for a given column of the *x*-signature (Hong, Wan, and Jain, 1998). The *x*-signature on the right clearly exhibits five peaks; the four distances between consecutive peaks are averaged to determine the local ridge frequency.

Estimation of Local Ridge Frequency

Simple Algorithm

1) 32x16 oriented window centered at $[x_i, y_i]$

2) The x-signature of the grey levels is obtained

3) f_{ij} is the inverse of the average distance

To handle noise interpolation and/or low pass filtering is applied.

DEMO: **Fp1 = computelocalfrequency(Fp1, Fp1.imOriginal);**

laboratory Gerstner

Estimation of Local Ridge Frequency

- Example on Variation Function Tech.

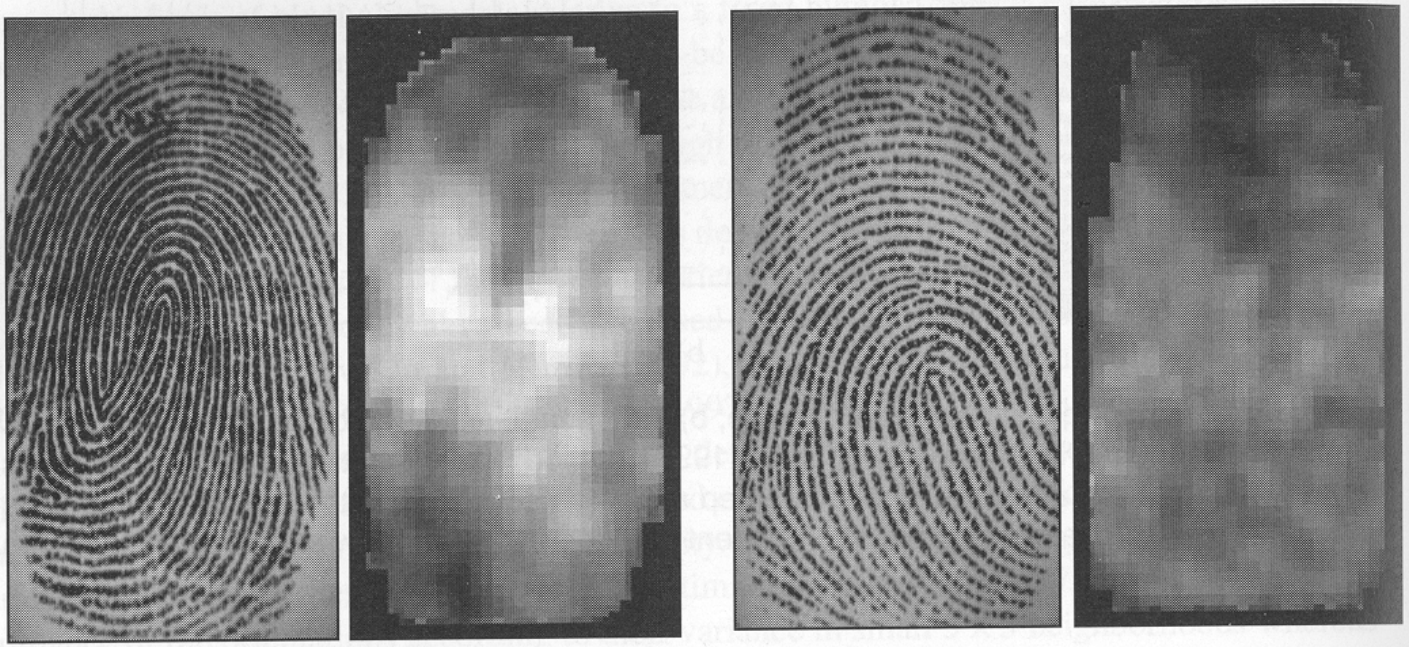

Figure 3.10. Two fingerprint images and the corresponding frequency image computed with the method proposed by Maio and Maltoni (1998a). A local 3×3 averaging is performed after frequency estimation to reduce noise. Light blocks denote higher frequencies. It is quite evident that significant changes may characterize different fingerprint regions and different average frequencies may result from different fingers.

Enhancement

- Performance depends on quality of images, 10% b) & c)
- Ideal fingerprint
- Degradation types – ridges are not continuous, parallel ridges are not well separated, cuts/creases/bruises
- Leads to problems in minutiae extraction

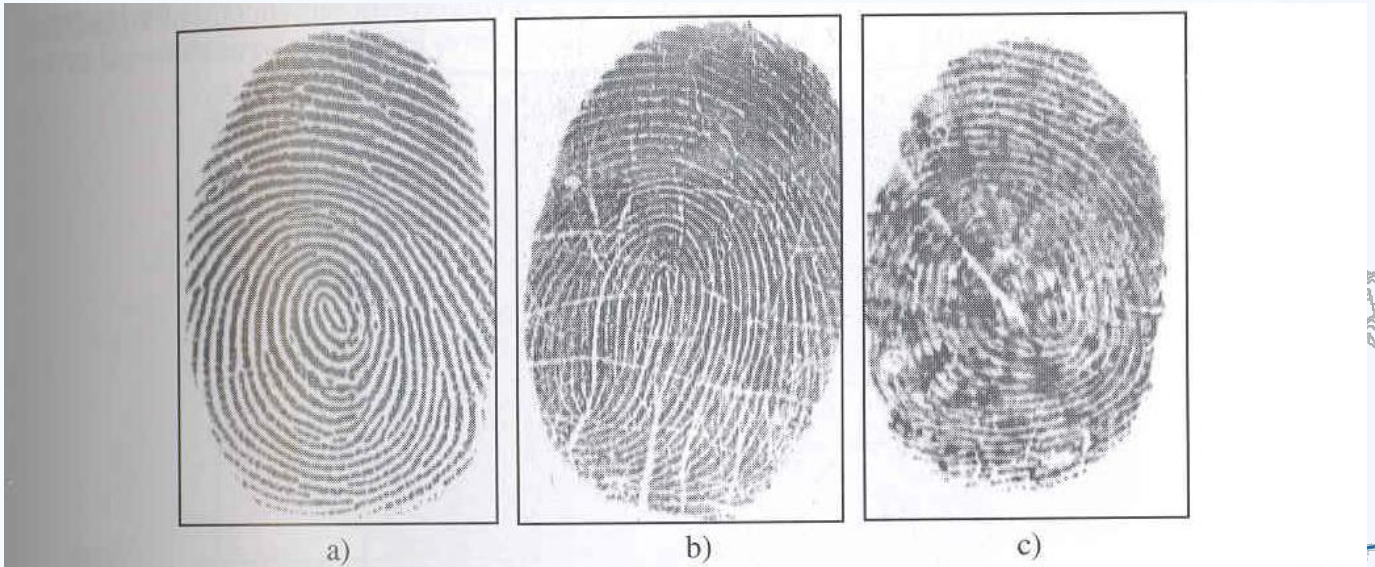

Figure 3.23. a) A good quality fingerprint; b) a medium quality fingerprint characterized by scratches and ridge breaks; c) a poor quality fingerprint containing a lot of noise.

Enhancement

For each fingerprint image, the fingerprint areas resulting from segmentation can be divided into:

- Well-defined region
- Recoverable region
- Unrecoverable region

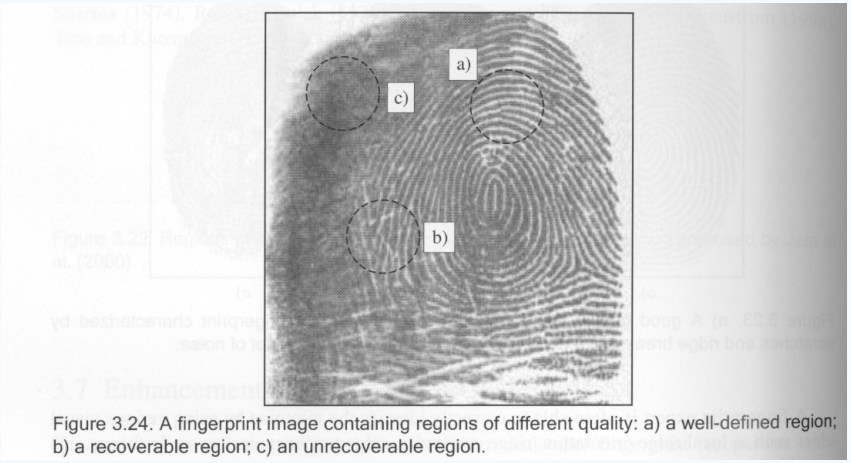

Figure 3.24. A fingerprint image containing regions of different quality: a) a well-defined region; b) a recoverable region; c) an unrecoverable region.

Enhancement

- Goal – to improve the clarity of the ridge structure in the recoverable regions and mark unrecoverable regions as too noisy for further processing
- Input – a gray-scale image
- Output – a gray-scale or binary image depending on the algorithm
- Effective initial steps - Contrast stretching, Histogram manipulation, Normalization, Wiener Filtering

laboratory Gerstner

Normalization approach [Hong, Wan, Jain (1998)]

- Determines the new intensity value of each pixel as,

$$\mathbf{I}'[x,y] = \begin{cases} m_0 + \sqrt{(\mathbf{I}[x,y]-m)^2 \cdot v_0 / v} & \text{if } \mathbf{I}[x,y] > m \\ m_0 - \sqrt{(\mathbf{I}[x,y]-m)^2 \cdot v_0 / v} & \text{otherwise,} \end{cases}$$

m and v - image mean and variance

m_0 and v_0 - desired values after normalization

- Pixel-wise operation, does not change the ridge and valley structures

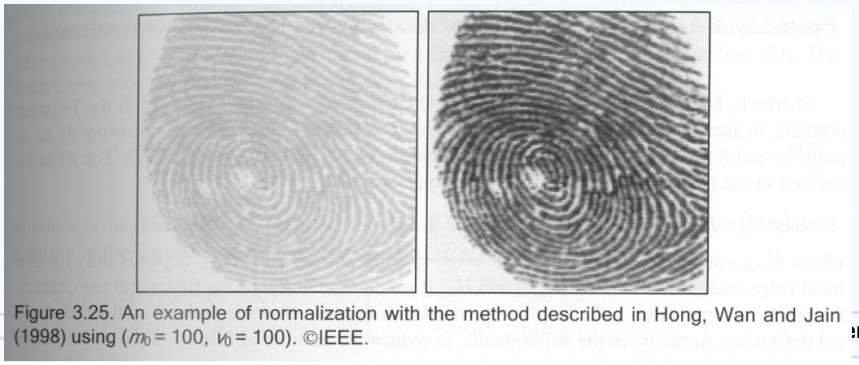

Figure 3.25. An example of normalization with the method described in Hong, Wan and Jain (1998) using ($m_0 = 100$, $v_0 = 100$). ©IEEE.

Contextual Filters

- The most widely used technique for fingerprint image enhancement
- Conventional image filtering – a single filter is used for convolution throughout
- Contextual filtering - filter characteristics change according to local context
- Several types of contextual filters proposed
- Indented behavior –
  - 1)provide a low-pass [averaging] effect along the ridge direction. *Linking small gaps and filling impurities due to noise*
  - 2)perform a band pass [differentiating] in the direction orthogonal to the ridges
    Increase discrimination between ridges and valleys

laboratory Gerstner

Method proposed by Hong, Wan, and Jain

- Based on Gabor filters
- Gabor filters have both frequency-selective and orientation-selective properties and have optimal joint resolution in spatial and frequency domains
- A Gabor filter is defined by a sinusoidal plane wave tapered by a Gaussian

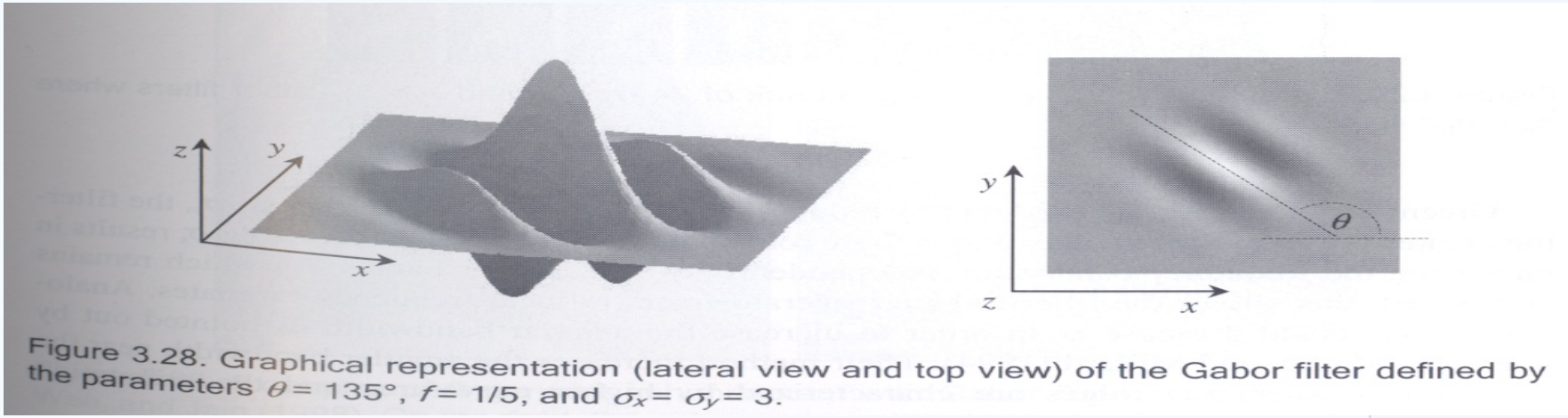

Figure 3.28. Graphical representation (lateral view and top view) of the Gabor filter defined by the parameters $\theta = 135°$, $f = 1/5$, and $\sigma_x = \sigma_y = 3$.

Method proposed by Hong, Wan, and Jain (cont ..)

The even symmetric two-dimensional Gabor filter has the following form:

$$g(x, y : \theta, f) = \exp\left\{-\frac{1}{2}\left[\frac{x_\theta^{\,2}}{\sigma_x^{\,2}} + \frac{y_\theta^{\,2}}{\sigma_y^{\,2}}\right]\right\} \cdot \cos(2\pi f \cdot x_\theta), \qquad (5)$$

where θ is the orientation of the filter, and $[x_\theta, y_\theta]$ are the coordinates of $[x,y]$ after a clockwise rotation of the Cartesian axes by an angle of $(90°-\theta)$.

$$\begin{bmatrix} x_\theta \\ y_\theta \end{bmatrix} = \begin{bmatrix} \cos(90° - \theta) & \sin(90° - \theta) \\ -\sin(90° - \theta) & \cos(90° - \theta) \end{bmatrix} \begin{bmatrix} x \\ y \end{bmatrix} = \begin{bmatrix} \sin\theta & \cos\theta \\ -\cos\theta & \sin\theta \end{bmatrix} \begin{bmatrix} x \\ y \end{bmatrix}.$$

Here, f is the frequency of a sinusoidal plane wave and σ_x and σ_y are the standard deviations of the Gaussian envelope along the x and y axes

Method proposed by Hong, Wan, and Jain (cont ..)
Gabor Filter

- 4 parameters – θ ,f, σ_x, σ_y
- The selection of the values σ_x and σ_y involves a tradeoff
- A set $\{g_{ij}(x,y) \mid i=1...n_0, 1..n_f\}$ of filters are priori created and stored , where n_0 is the number of discrete orientations $\{\theta_i \mid i=1,..n_0\}$ and n_f the number of discrete frequencies $\{f_j \mid j=1,..n_f\}$
- Each pixel [x,y] is convolved, with filter $g_{ij}(x,y)$ such that θ_i is the discretized orientation closest to θ_{xy} and f_j is the discretized orientation closest to f_{xy}
- **DEMO: Fp1 = enhance2ridgevalley(Fp1);**

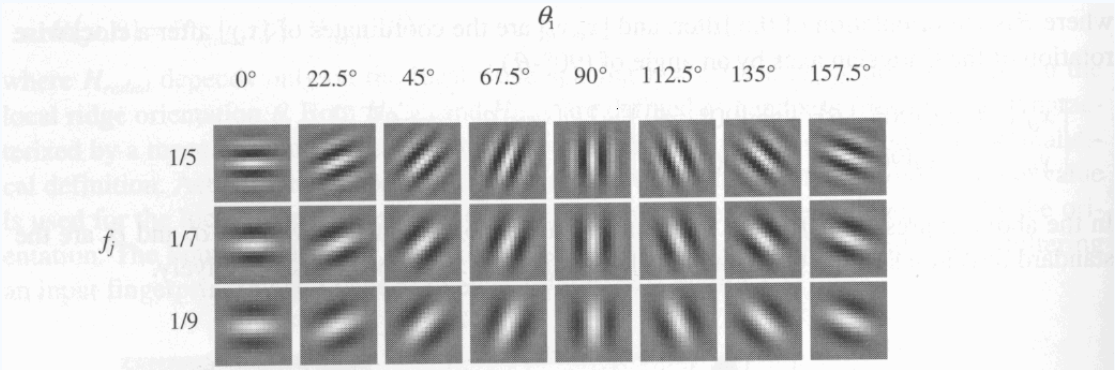

Figure 3.29. A graphical representation of a bank of 24 (n_o = 8 and n_f = 3) Gabor filters where $\sigma_x = \sigma_y = 4$.

Method proposed by Hong, Wan, and Jain (cont ..) – Examples

- Shows the application of Gabor-based contextual filtering on medium and poor quality images

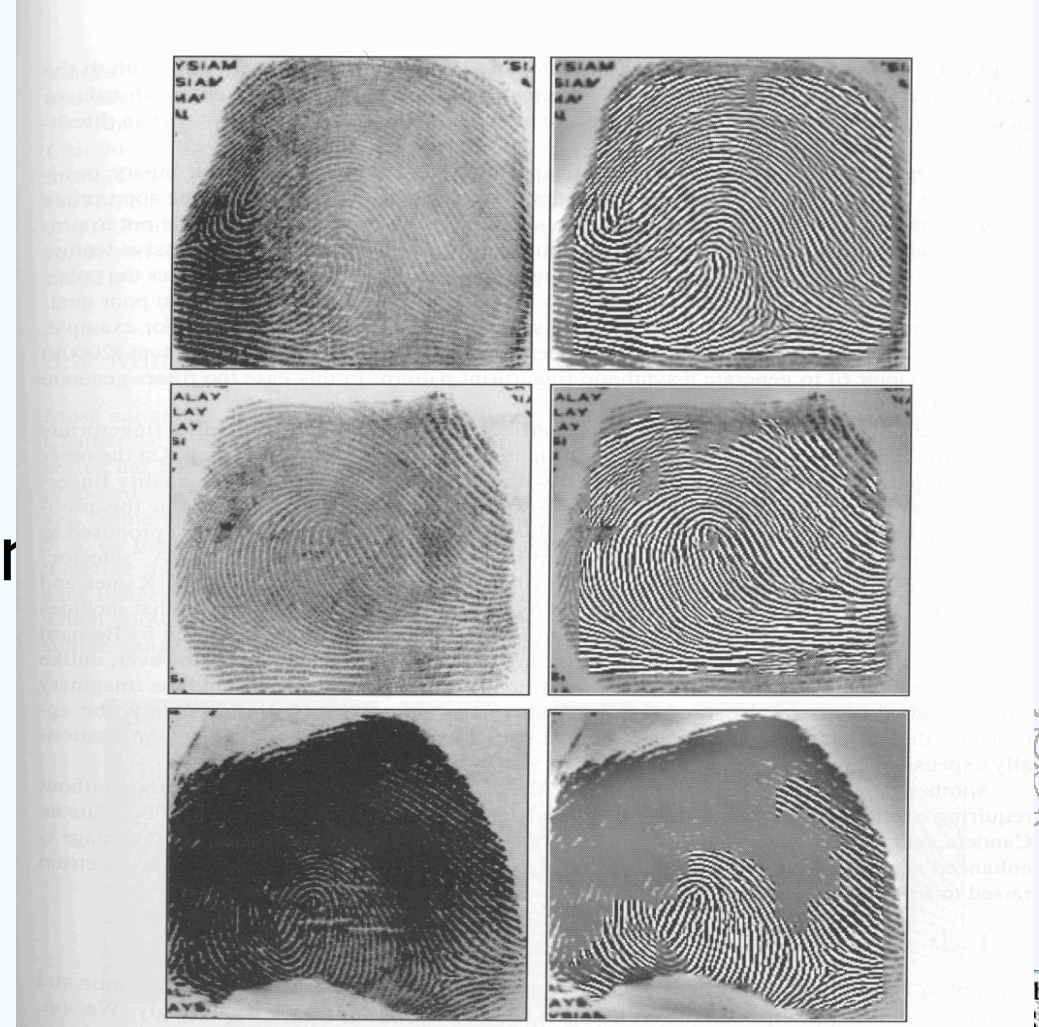

Figure 3.30. Examples of fingerprint enhancement with Gabor filtering as proposed by Hong, Wan, and Jain (1998). On the right, the enhanced recoverable regions are superimposed on the corresponding input images. ©IEEE.

Minutiae Detection

- Reliable minutiae extraction is extremely important
  - Binarization
  - Thinning
  - Post processing – filling holes, linking breaks, removing bridges

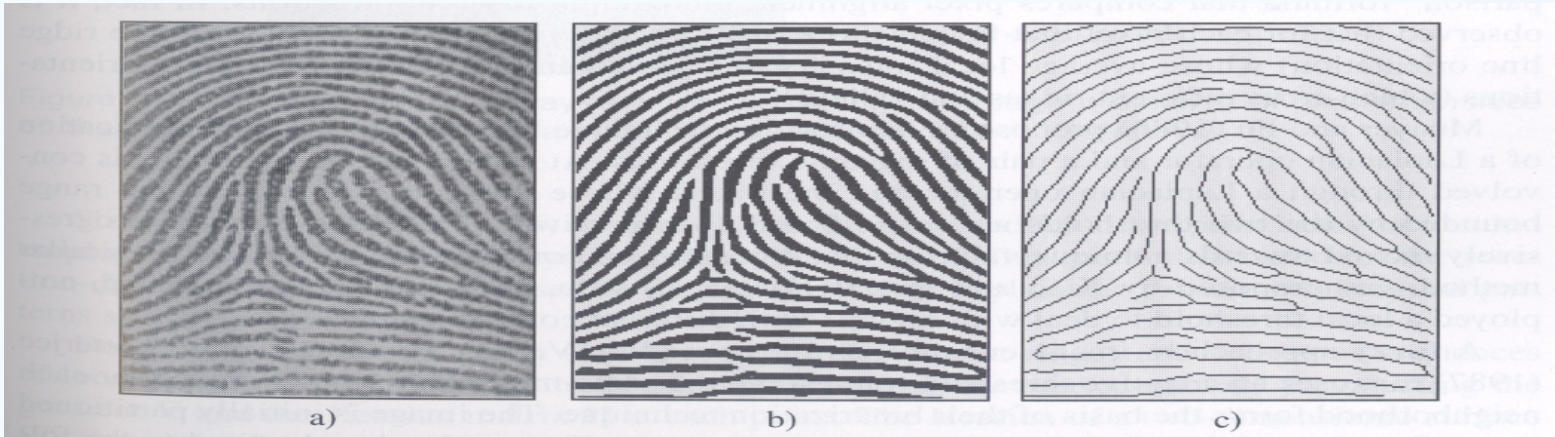

Figure 3.31. a) A fingerprint gray-scale image; b) the image obtained after a binarization of the image in a); c) the image obtained after a thinning of the image in b). Reprinted with permission from Maio and Maltoni (1997). ©IEEE.

Binarization-based methods

- Simplest method - global threshold
- Local threshold technique
- Fingerprint specific solutions necessary

- Binarization is the output of Contextual Filtering: **enhance2ridgevalley.m**

```
binaryBlkSize = 20;
imReconstruct = blkproc(imReconstruct, [binaryBlkSize
   binaryBlkSize], @binarizeimage);

function  Iout = binarizeimage(Iin)
level = graythresh(Iin); %Otsu method
Iout = im2bw(Iin, level);
```

laboratory Gerstner

Threshold computation: Otsu I

- Otsu's method: *N. Otsu (1979). "A threshold selection method from gray-level histograms". IEEE Trans. Sys., Man., Cyber. 9: 62–66*
  - *http://en.wikipedia.org/wiki/Otsu%27s_method*
  - *http://homepages.inf.ed.ac.uk/rbf/CVonline/LOCAL_COPIES/MORSE/threshold.pdf*
- minimizes the intra-class variance – for each threshold T lot's of work

$$\sigma^2_{\text{Within}}(T) = n_B(T)\sigma^2_B(T) + n_O(T)\sigma^2_O(T)$$

- between-class variance:

$$\sigma^2_{\text{Between}}(T) = \sigma^2 - \sigma^2_{\text{Within}}(T) = n_B(T)\left[\mu_B(T) - \mu\right]^2 + n_O(T)\left[\mu_O(T) - \mu\right]^2$$

$$n_B(T) = \sum_{i=0}^{T-1} p(i)$$

$$n_O(T) = \sum_{i=T}^{N-1} p(i)$$

$\sigma^2_B(T)$ = the variance of the pixels in the background (below threshold)

$\sigma^2_O(T)$ = the variance of the pixels in the foreground (above threshold)

where σ^2 is the combined variance and μ is the combined mean

Threshold computation: Otsu II

- Compute histogram and probabilities of each intensity level
- Set up initial $n_b(0)$ and $n_o(0)$ and $\mu_b(0)$, $\mu_o(0)$
- Step through all possible thresholds T=1.... maximum intensity
  - Update $n_b(T)$,$n_o(T)$
  - Compute $\sigma_{between}(T)$
- Desired threshold corresponds to the maximum $\sigma_{between}(T)$

laboratory Gerstner

Minutiae detection

- A simple image scan allows the pixel corresponding to minutiae to be detected
- *crossing number* of a pixel p
- **DEMO: Fp1 = cleanskeleton(Fp1);**

$$cn(\mathbf{p}) = \frac{1}{2}\sum_{i=1..8} \left| val(\mathbf{p}_{i \bmod 8}) - val(\mathbf{p}_{i-1}) \right|,$$

where $\mathbf{p}_0, \mathbf{p}_1, \ldots, \mathbf{p}_7$ are the pixels belonging to an ordered sequence of pixels defining the 8-neighborhood of $\mathbf{p}$ and $val(\mathbf{p}) \in \{0,1\}$ is the pixel value. It is simple to note (Figure 3.36) that a pixel $\mathbf{p}$ with $val(\mathbf{p}) = 1$:

- is an intermediate ridge point if $cn(\mathbf{p}) = 2$;
- corresponds to a termination minutia if $cn(\mathbf{p}) = 1$;
- defines a more complex minutia (bifurcation, crossover, etc.) if $cn(\mathbf{p}) \geq 3$.

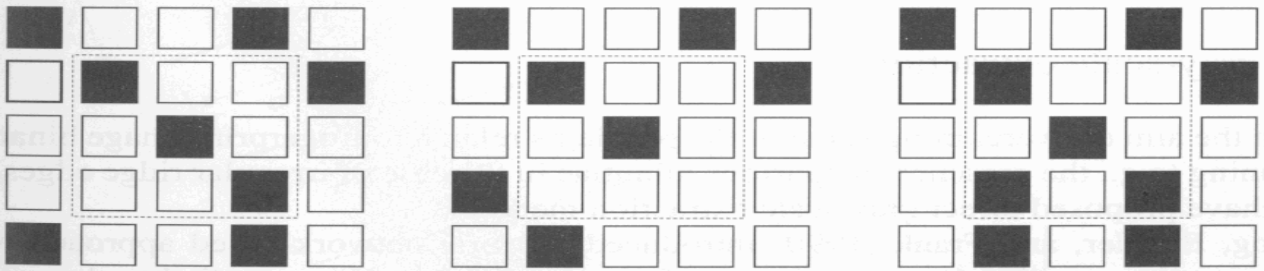

a) $cn(\mathbf{p}) = 2$ b) $cn(\mathbf{p}) = 1$ c) $cn(\mathbf{p}) = 3$

Figure 3.36. a) intra-ridge pixel; b) termination minutia; c) bifurcation minutia.

Examples of minutiae extraction

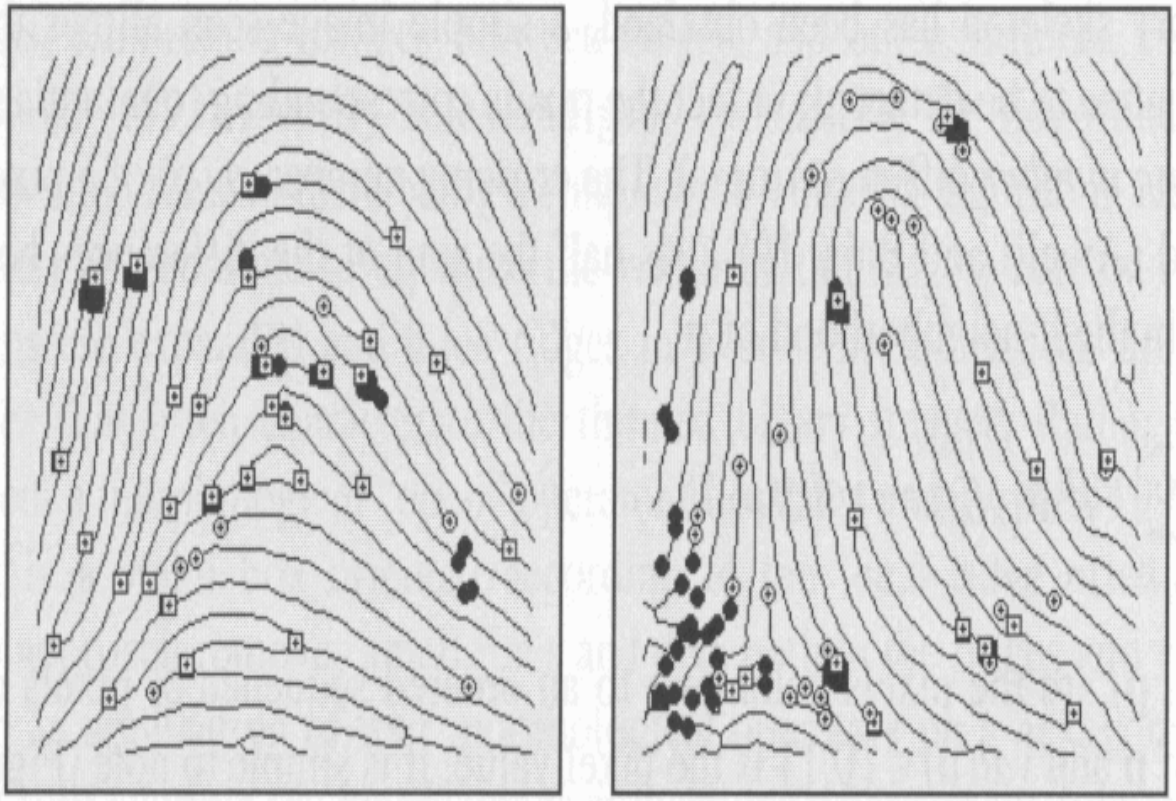

Figure 3.37. Examples of minutiae detection on binary skeletons. White circles and white boxes denote terminations and bifurcations, respectively; black circles and black boxes denote filtered minutiae (see Section 3.9).

Direct gray-scale extraction

Such methods are used to overcome the problems related to fingerprint binarization and thinning [e.g. spurious minutiae]

Maio and Maltoni (1997)

- Basic idea – track the ridge lines in the gray-scale image, by “sailing” according to the local orientation of the ridge pattern
- A ridge line is defined as a set of points that are local maxima along one direction
- The ridge line extraction algorithm tries to locate the local maximum relative to a section orthogonal to the ridge direction
- A polygonal approximation of the ridge line can be obtained by connecting the consecutive maxima

Ridge line following algorithm - steps

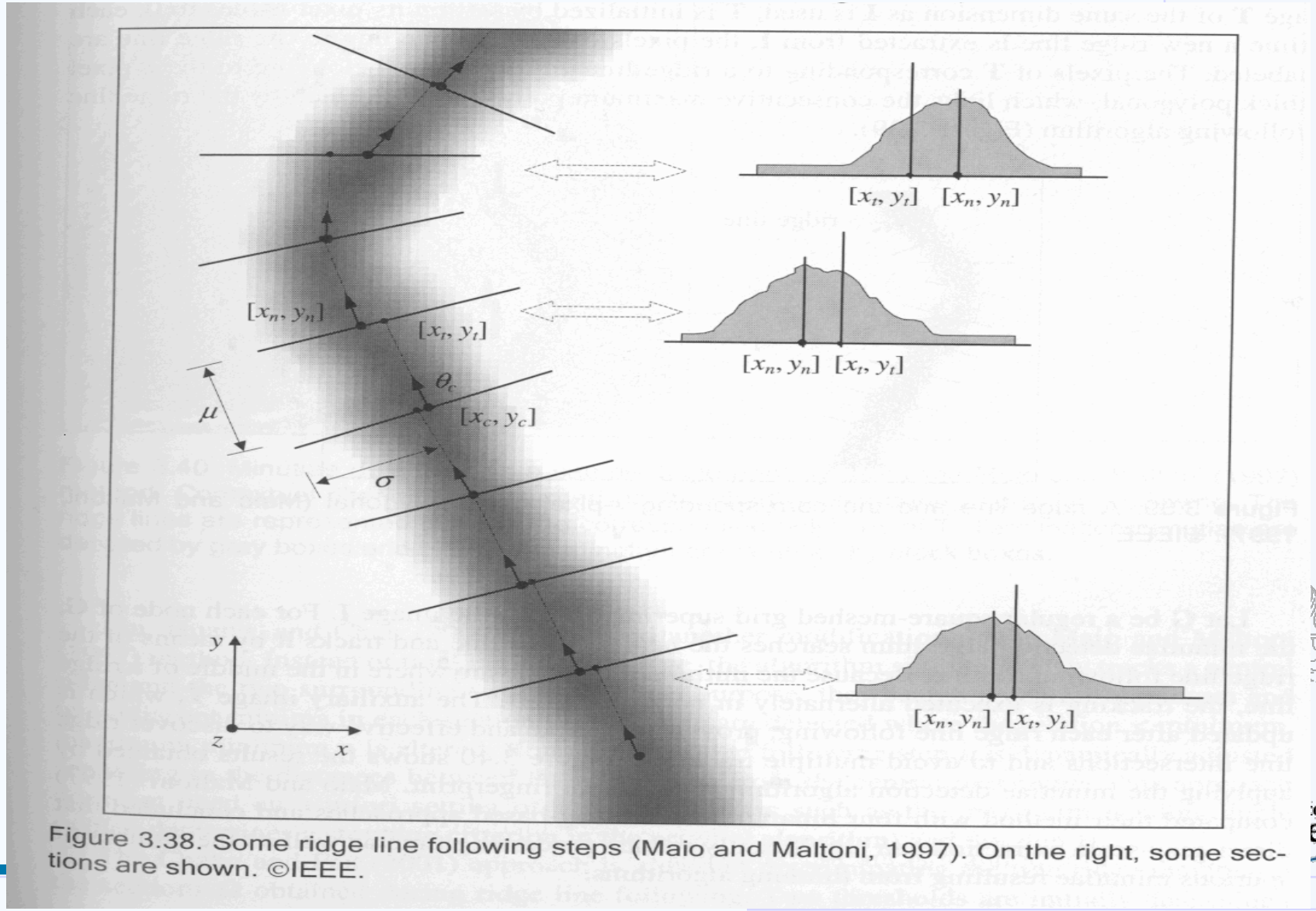

Figure 3.38. Some ridge line following steps (Maio and Maltoni, 1997). On the right, some sections are shown. ©IEEE.

Ridge line following – algorithm (pseudo-code version)

- Let (i_s,j_s) be a local maximum of a ridge line of I
- Φ_0 be the direction of the tangent to the ridge line in (i_s,j_s)
- Parameters to be set – σ,μ

```
ridge line following(i_s, j_s, φ_0)
  { end := false ;
    (i_c , j_c ) := (i_s , j_s );
    φ_c := φ_0 ;
    while (¬ end)
      { (i_t , j_t ) := (i_c , j_c ) + μ pixel
          along direction φ_c ;
        Ω := section set centered in
            (i_t, j_t) with direction φ_c+π/2
            and length 2σ+1;
        (i_n , j_n ) := local maximum over Ω ;
        store (i_n , j_n ) ;
        end := check stop criteria on
           (i_c , j_c ), (i_t , j_t ), (i_n , j_n ) ;
        ( i_c , j_c ) := ( i_n , j_n ) ;
        φ_c := tangent direction in (i_c , j_c
);
      }
  }
```

laboratory Gerstner

cal University

Results of minutiae detection algorithm on a sample fingerprint

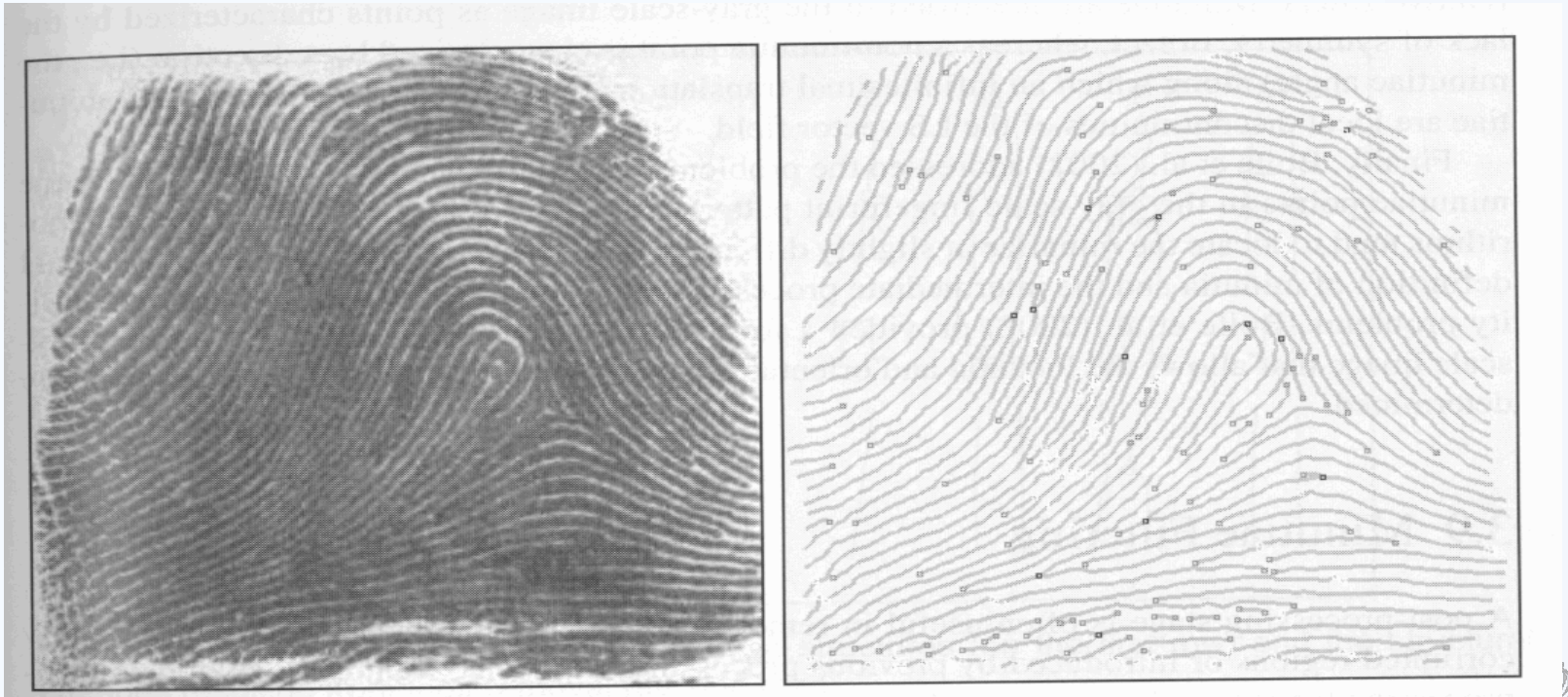

Figure 3.40. Minutiae detection on a sample fingerprint by using the Maio and Maltoni (1997) method. Contextual filtering is performed on "touched" pixels during ridge line following. The ridge lines are represented through the corresponding polylines of T. Termination minutiae are denoted by gray boxes and bifurcation minutiae are denoted by black boxes.

Minutiae Filtering

- Post-processing stage is useful for removing spurious minutiae [already present or introduced by previous steps]
- Two main post-processing types:
  - Structural post-processing
  - Minutiae filtering in the gray-scale domain

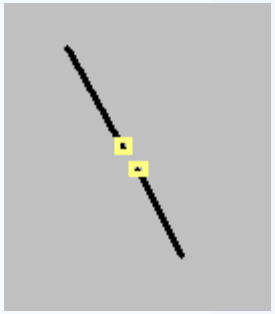

- Ridge breaks (insufficient ink or moist)

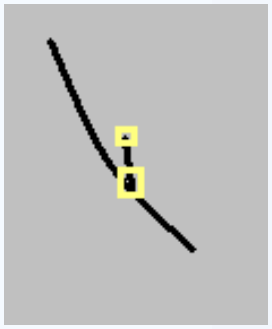

- Ridge cross-connections (over-ink, over-moist)

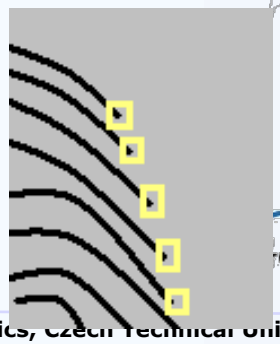

- Boundaries

Example

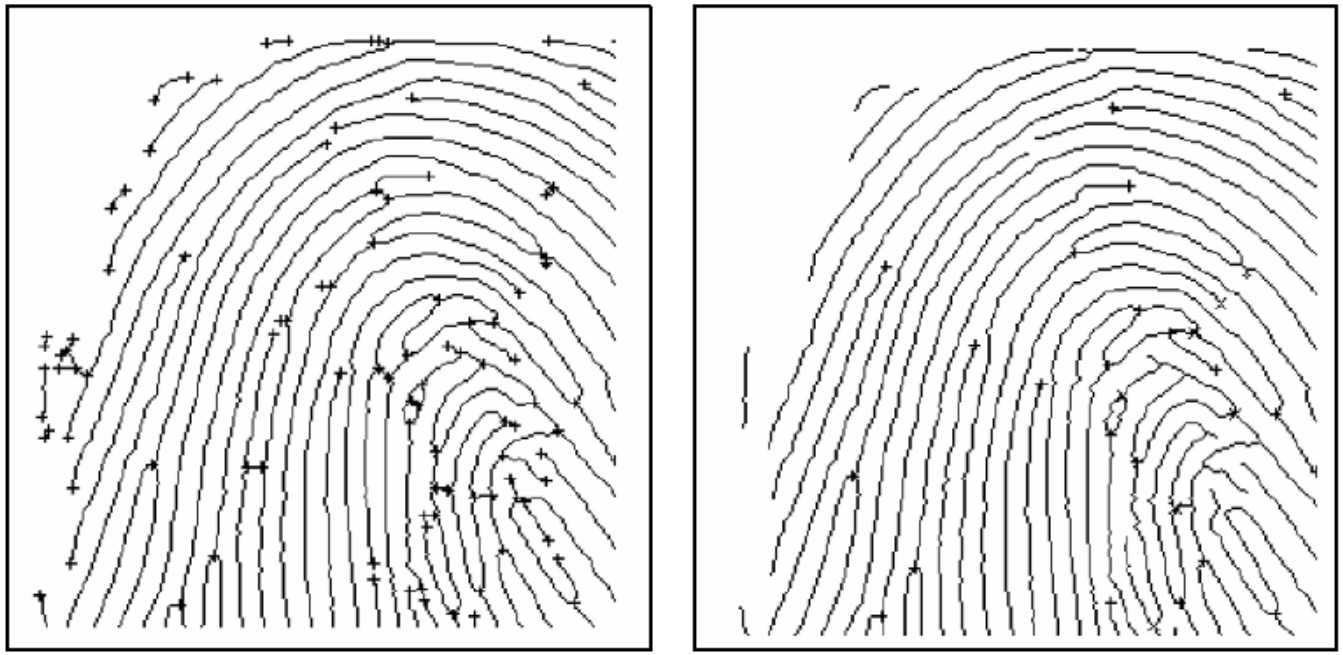

Figure 3.51. Minutiae post-processing according to Farina, Kovacs-Vajna, and Leone (1999). On the right, most of the false minutiae present in the thinned binary image (on the left) have been removed. © Elsevier.

Structural post-processing

- Xiao and Raafat (1991) identified the most common false minutiae structures and introduced an ad hoc approach
- The underlying algorithm is rule-based
- Requires as input – length of the associated ridge(s), the minutia angle, the number of facing minutiae in a neighborhood

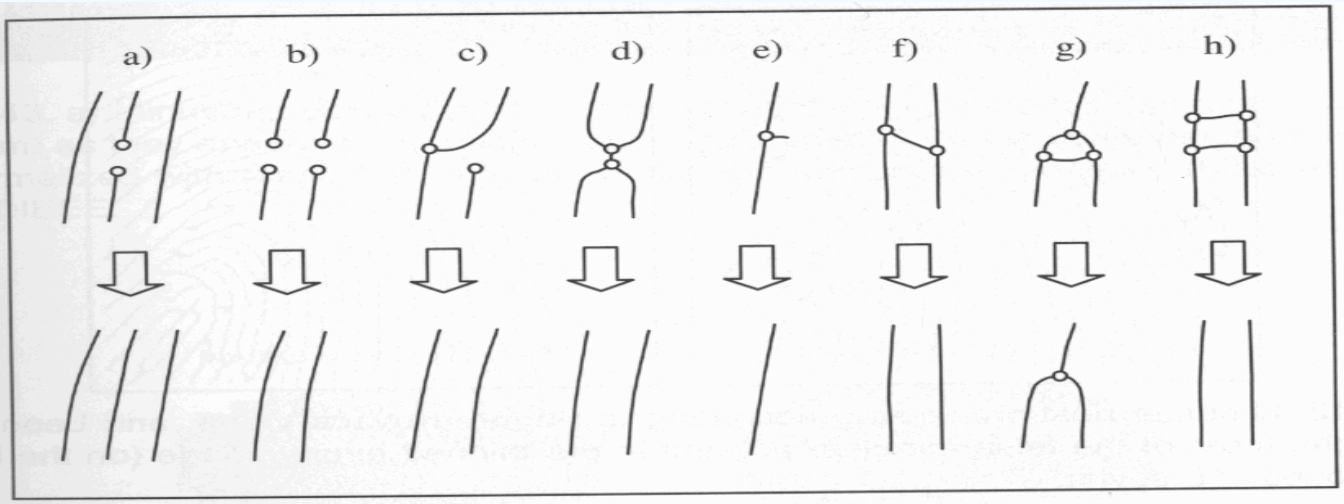

Figure 3.41. The most common false-minutiae structures (on the first row) and the structural changes resulting from their removal (second row).

Minutiae filtering in gray-scale domain

- A direct minutiae filtering technique reexamines the gray-scale image in a spatial neighborhood of a detected minutiae with the aim of verifying the presence of a real minutia
- Maio and Maltoni used a shared weight neural network to verify the minutiae detected by their gray-scale algorithm
- The minutiae neighborhoods are normalized with respect to their angle and the local ridge frequency

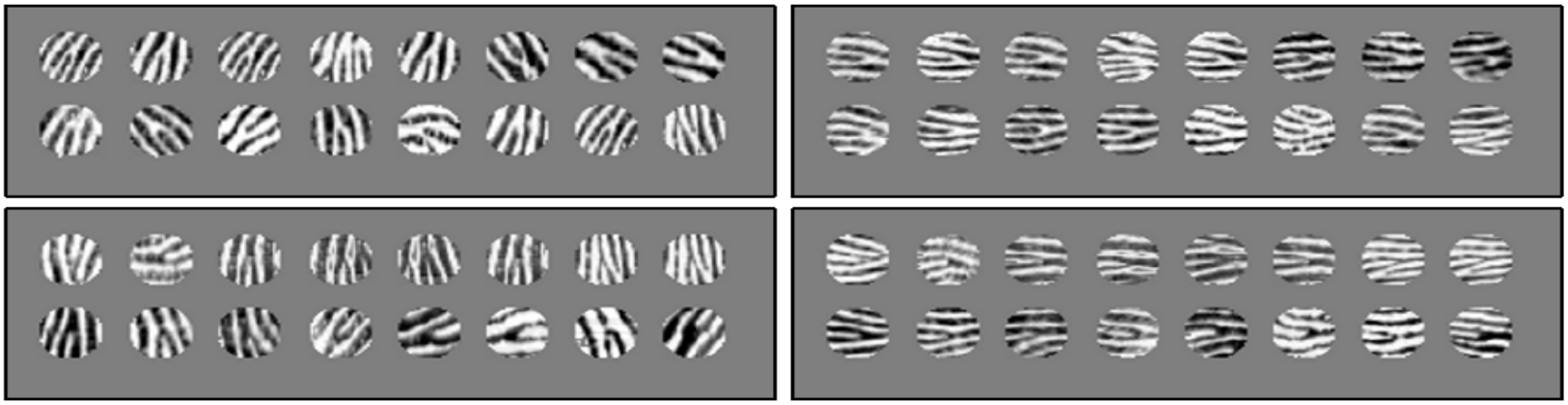

Figure 3.52. a) Minutiae neighborhoods (ridge ending minutiae at the top, bifurcation minutiae at the bottom) as they appear in the original gray-scale images; b) the same neighborhoods have been normalized with respect to minutiae angle and local ridge frequency (Maio and Maltoni, 1998b). © IEEE.

Minutiae filtering in gray-scale domain

- Then they are passed to a neural network classifier, which classifies them as termination, bifurcation and non-minutia
- A typical three layer neural network architecture has been adopted

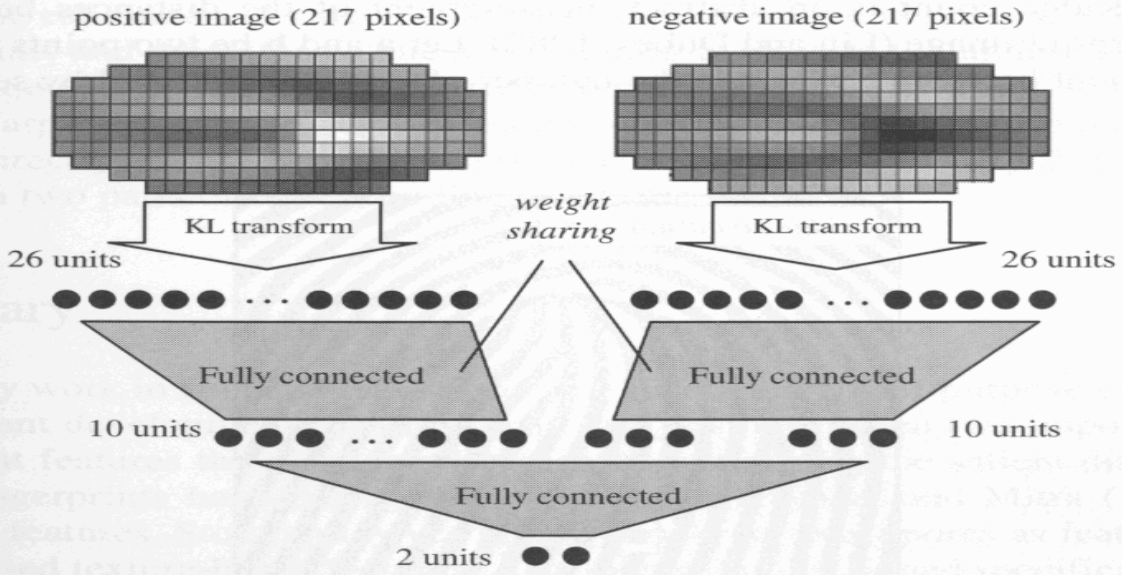

Figure 3.44. The neural network architecture to classify gray-scale minutiae neighborhoods into termination, bifurcation, and non-minutiae (Maio and Maltoni, 1998b). ©IEEE.

Estimation of ridge count

- *ridge count* has often been used to increase reliability of analysis
- Ridge count is an abstract measurement of the distances between any two points in a fingerprint image
- Typically used in forensic matching: counting between core and delta

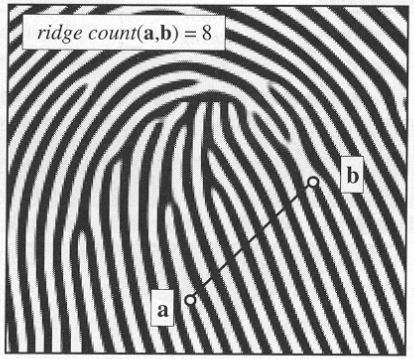

Figure 3.45. In this example the number of ridges intersected by segment **ab** (ridge count between **a** and **b**) is 8.